Effect of calcium source on structure and properties of sol-gel derived bioactive glasses

Bobo Yu[1], Claudia A. Turdean-Ionescu[2], Richard A. Martin[3], Robert J. Newport[4], John V. Hanna[2], Mark E. Smith[2,5], Julian R. Jones[1]

[1] Department of Materials, Imperial College London, London, SW7 2AZ, UK

[2] Department of Physics, University of Warwick, Coventry, CV4 7AL, UK

[3] School of Engineering & Applied Science and Aston Research Centre for Healthy Ageing, Aston University, Birmingham, B4 7ET, UK

[4] School of Physical Science, University of Kent, Canterbury, CT2 7NH, UK

[5]Vice-Chancellor's Office, University House, Lancaster University, LA1 4YW, UK.

KEYWORDS: bioactive glass; biomaterials; sol-gel; inorganic/organic hybrids; calcium methoxyethoxide

ABSTRACT

The aim was to determine the most effective calcium precursor for synthesis of sol-gel hybrids and for improving homogeneity of sol-gel bioactive glasses. Sol-gel derived bioactive calcium silicate glasses are one of the most promising materials for bone regeneration. Inorganic/organic hybrid materials, which are synthesized by incorporating a polymer into the sol-gel process, have also recently been produced to improve toughness. Calcium nitrate is conventionally used as the calcium source but it has several disadvantages. Calcium nitrate causes inhomogeneity by forming calcium-rich regions and it requires high temperature treatment (>400 °C) for calcium to be incorporated into the silicate network. Nitrates are also toxic and need to be burnt off. Calcium nitrate therefore cannot be used in the synthesis of hybrids as the highest temperature used in the process is typically 40-60 °C. Therefore, a different precursor is needed that can incorporate calcium into the silica network and enhance the homogeneity of the glasses at low (room) temperature. In this work, calcium methoxyethoxide (CME) was used to synthesize sol-gel bioactive glasses with a range of final processing temperatures from 60 to 800 °C. Comparison is made between the use of CME and calcium chloride and calcium nitrate. Using advanced probe techniques, the temperature at which Ca is incorporated into the network was identified for 70S30C (70 mol% SiO_2, 30 mol% CaO) for each of the calcium precursors. When $CaCl_2$ was used, the Ca did not seem to enter the network at any of the temperatures used. In contrast, Ca from CME entered the silica network at room temperature, as confirmed by XRD, ^{29}Si Magic Angle Spinning Nuclear Magnetic Resonance spectroscopy and dissolution studies. CME should be used in preference to calcium salts for hybrid synthesis and may improve homogeneity of sol-gel glasses.

1. Introduction

Bioactive glasses bond with bone and are osteogenic [1]. However they are brittle, therefore hybrids are being developed with the aim of introducing toughness while maintaining the bioactive properties of the glass [2, 3]. The bond with bone is thought to be due to their reaction with body fluid, which results in the formation of a hydroxy carbonate apatite (HCA) surface layer on the glass [4]. The first sol-gel bioactive glasses were prepared in the early 1990s for bone regeneration [5]. The inherent nanoscale porosity of the sol-gel process significantly increases the surface area of these glasses [6], which enhances the rates of apatite phase formation and bone bonding, together with controlled degradation/resorption properties. Foaming of sol-gel solutions has been performed to produce three-dimensional (3D) scaffolds that provide an interconnected macroporous network for cell migration, vascularization and bone ingrowth [7, 8]. The foaming process uses a surfactant to stabilize the air bubbles and produce pores and hydrofluoric acid (HF) as a catalyst for rapid gelation of the silica network.

In a sol-gel glass a silica network forms by a condensation reaction under constant stirring [9-11]. Inhomogeneity in the structure appears when using the conventional $Ca(NO_3)_2 \bullet 4H_2O$ source for calcium. Lin *et al.* reported Ca-rich regions at the edges of large monoliths [12]. This is due to the $Ca(NO_3)_2$ being soluble in the pore liquor (the by-product of the condensation reaction) during the gelation and aging stages. This liquid is then expelled out of the gel due to the shrinkage. During drying, the pore liquor evaporates leaving $Ca(NO_3)_2$ deposits on the outer parts of the monolith. The calcium only enters the silicate network above 400 °C [13-14] by diffusion above this temperature, but can only diffuse a limited distance during thermal stabilization [14]. In foams,

where diffusion distances into the struts are short, homogeneity is improved, although a calcium distribution can be observed using synchrotron X-ray microtomography [15]. Strontium ions are thought to be beneficial for patients with osteoporosis and strontium has been introduced into the sol-gel glass composition using strontium nitrate, therefore Sr distribution may also be affected by diffusion distances and the type of precursor [16].One aim of this work is to improve the homogeneity of calcium in sol-gel glass monoliths.

In order to induce toughness in sol-gel glasses, inorganic/organic hybrids that have interpenetrating networks of silica and biodegradable polymers can be synthesized. Hybrids are synthesized by introducing a polymer into the sol-gel process so that the silica network and polymer form interpenetrating networks at the nanoscale [3, 17-19]. While calcium nitrate has been used in hybrid synthesis [20], it did not enter the network during processing at the lower temperatures [14] and is therefore not an ideal calcium precursor.

Since calcium is intrinsic to the bioactivity of the sol-gel glasses, there is a need to find an alternate Ca precursor that will introduce Ca into the silica network at room temperature, improving the homogeneity of sol-gel derived bioactive glasses and allowing hybrid synthesis [1]. One option is an alternative calcium salt with less toxic by-products, e.g. calcium chloride [18, 21] or calcium acetate. Another option is to use a calcium alkoxide, such as calcium methoxyethoxide (CME). Pereira *et al.* were the first to use CME to synthesize sol-gel derived bioactive glasses, synthesizing three compositions in the CaO-P_2O_5-SiO_2 system; S60 (60% SiO_2, 36% CaO and 4% P_2O_5), S70 (70% SiO_2, 26% CaO and 4% P_2O_5) and S80 (80% SiO_2, 16% CaO and 4% P_2O_5) [22]. All compositions formed an HCA layer in TRIS and in SBF within 12 h. Ramila found that

using CME produced a more uniform HCA layer on glasses compared to that formed on glasses made with calcium nitrate [23]. However all these glasses were stabilized at 700 °C. CME was used in star gel synthesis where the final drying temperature was 90 °C [24]. Star gels are particular types of hybrids that have an organic core surrounded by flexible arms that terminate with alkoxysilane groups. The silica content of these materials is therefore low. Recently CME was used in the synthesis of electrospun silica/ polylactide (PLLA) hybrids, but again, the silica network was a small percentage of the material [25]. The potential for calcium incorporation into a silica network at low temperature was not assessed.

The aim of this work is to investigate the use of different calcium precursors for low temperature (<130 °C) sol-gel synthesis to assess their potential for the production of bioactive hybrids. The hypothesis was that CME would improve the incorporation of calcium into the sol-gel silica network at low temperature compared to the traditional method of using calcium salts. To achieve this, advanced probe techniques were employed to compare the effect of calcium precursor type on calcium incorporation in 70S30C and on their subsequent dissolution. To understand the mechanism of calcium incorporation, a range of sol-gel stabilization studies were used. The effect of HF was also investigated because, in porous scaffold production, HF is used to rapidly gel silica sols during foaming [7]. HF forms a complex with the silica, increasing the rate of bridging oxygen bond formation. It is therefore important to assess whether alternative calcium precursors modify the silica network formed by the action of HF [26].

2. Materials and Methods

2.1 Sample preparation

Glasses were made of the bioactive 70S30C (70 mol% SiO_2, 30 mol% CaO) composition. Three calcium precursors ($Ca(NO_3)_2$, $CaCl_2$ and CME) were used to produce each of the glasses. Calcium acetate was also used in pilot studies. Sol-gel solutions were gelled with and without hydrofluoric acid (HF) and different heat treatments were applied to the gelled samples.

Commercial calcium methoxyethoxide (CME) was found to have inconsistent properties (i.e. dependent on supplier and batch), so CME was prepared following the method described by Pickup *et al.*[27]: 1 g of calcium metal was reacted with 24 ml of 2-methoxyethanol under an argon atmosphere at 80 °C for 24 h. The resultant solution was centrifuged at 6000 rpm for 10 minutes to remove unreacted calcium metal. The concentration of CME in solution was confirmed gravimetrically by heating to 1050 °C for 12 h where the solvent evaporated and the CME converted to CaO. This revealed the CME solution concentration to be 0.001 mol/ml.

Calcium nitrate containing samples were synthesized using an established sol-gel method [28] (Figure 1, inorganic route). Deionised water and nitric acid (2N) were mixed together and stirred for 5 minutes followed by addition of tetraethyl orthosilicate (TEOS) into the mixture. The R ratio (molar ratio of water:TEOS) was 12. After 1 h, calcium nitrate tetrahydrate was added to the sol and the sol was stirred for a further hour. Sols were poured into moulds and sealed. Gelation was allowed to occur at room temperature. To investigate the effect of a gelation catalyst, HF was added to selected samples at a ratio of 1.5 ml of HF (0.5 w/v) to 50 ml of sol prior to pouring. Samples prepared without HF were left to complete gelation at room temperature for 3 days. For the preparation of the samples containing $CaCl_2$ as the calcium

precursor, the $Ca(NO_3)_2$ was replaced with $CaCl_2$ and 2N hydrochloric acid (HCl) was used in place of 2N HNO_3 to eliminate the nitrate by-products of HNO_3.

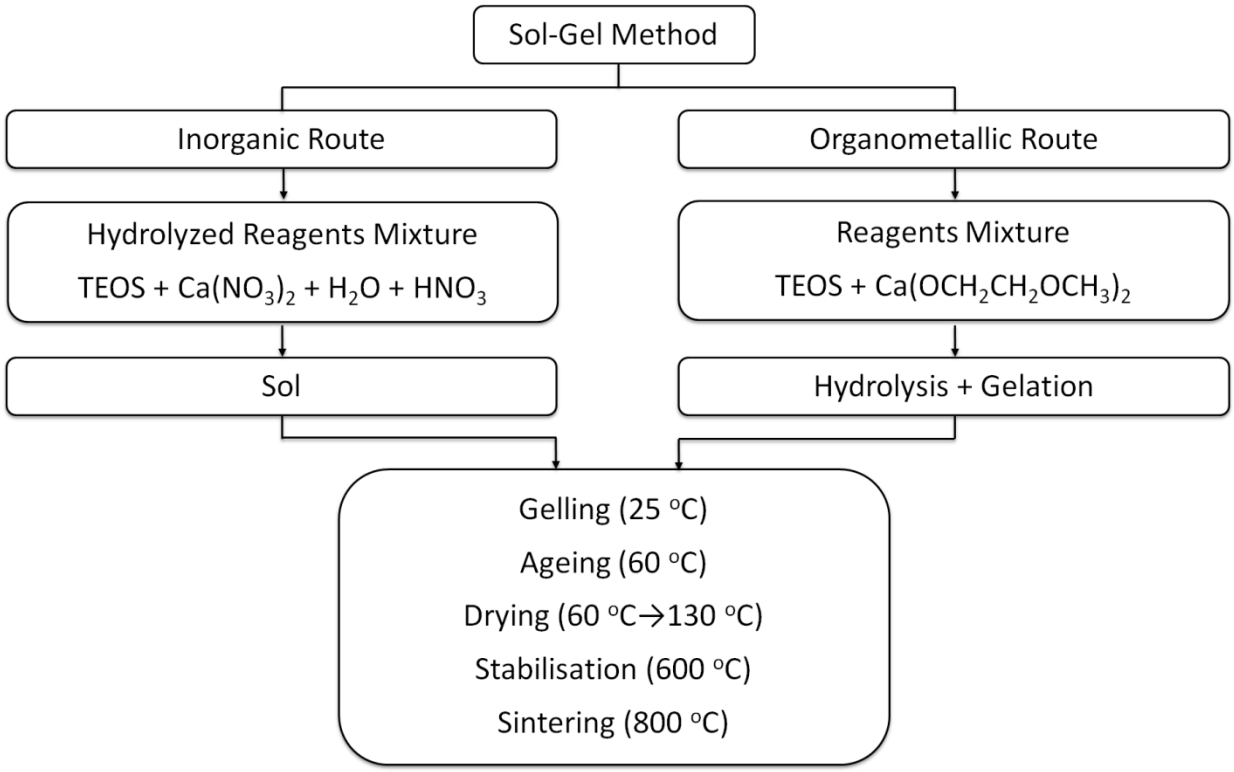

Figure 1. Flow chart of sol-gel methods used.

Synthesis with CME was performed by first mixing TEOS and CME under a nitrogen atmosphere (Figure 1, organic route). After 1h of being stirred, the sol was hydrolysed by mixing with water inside a hermetically sealed container. 250 ml of each sample was placed in a Teflon mould before heat treatment. The samples in the Teflon moulds were then left to age at room temperature for 3 days. Some of the $Ca(NO_3)_2$, $CaCl_2$ and CME samples were taken through the full sol-gel heat treatment (dried at 60-130 °C and stabilized at 700 °C with some sintered at 800 °C after stabilization) to enable direct comparison with conventional sol-gel glasses prepared via the nitrate route. The amounts of chemicals used to synthesize the samples are listed in Table 1.

All the resultant dry samples were ground to particle sizes of 38-90 μm. The glasses for the assessment of the calcium distribution were those dried at 130 °C (before stabilization); each sample was heated for one hour.

Table 1. Reagent quantities (ml) used to synthesize 250ml batches of sol.

Samples	H_2O [ml]	2N HNO_3 [ml]	2N HCl [ml]	TEOS [ml]	$Ca(NO_3)_2$ •$4H_2O$ [g]	$CaCl_2$ [g]	CME [ml]
70S30C-$Ca(NO_3)_2$	135.90	22.68	–	141.12	63.72	–	–
70S30C-$CaCl_2$	135.90	–	22.68	141.12	–	39.67	–
70S30C-CME	62.23	–	–	64.27	–	–	123.48

2.2 Characterization

Composition

The lithium metaborate fusion dissolution method was used in combination with inductive coupled plasma optical emission spectroscopy (ICP-OES) to determine the composition of the samples by measuring the ratio of Si and Ca [29]. The samples for this test were stabilized at 700 °C to remove moisture and 0.1 g of each sample was mixed with 0.5 g of anhydrous lithium metaborate in a clean dry platinum-gold crucible and fused at 1400 ˚C for 30 minutes. After cooling to room temperature, the crucible was immersed in a 250 ml beaker filled with 80 ml of 10 vol% nitric acid and stirred overnight with a magnetic stirrer. The solution was then transferred to a 100 ml polypropylene volumetric flask and filled up to the mark with 10 vol% nitric acid. The concentrations of Si, Ca, and P were then analyzed by ICP-OES (Thermo iCAP

6000). The proportions of SiO_2, CaO, and P_2O_5 were obtained by comparing the molar ratio of Si, Ca, and P.

Surface area and pore size

Meso-scale porosity was analyzed using nitrogen adsorption (Quantachrome AS6). The sol-gel frits were first degassed at room temperature over night to remove physically adsorbed gases, in particular water vapor. The surface area was calculated from the BET (Brunauer-Emmet-Teller) method [30] and pore size distributions determined by applying the BJH (Barrett-Joyner-Halenda) [31] method from the desorption branch of the isotherm [32].

Calcium distribution

The X-ray diffraction (XRD) data was collected using a Bruker D8 Advance X-ray diffractometer with an incident wavelength of 1.54 Å. The heat treatment was undertaken by placing the samples inside a preheated oven for 1 h before slowly cooling to room temperature. XRD patterns were obtained at a range of temperatures to determine the temperature at which Ca enters the silica network.

Dissolution tests were carried out to evaluate the release speed of Ca, P, and Si as a function of stabilization temperature. These temperatures were selected according to the results obtained from XRD patterns. The samples sieved into 38-90 μm were immersed into deionized water and then placed in a shaker at 37 °C, and an agitation rate of 120 rpm was used. At each time point (1, 2, 4, 8, 24, 72, 168, 336 and 672 h), 1 ml extracts were taken and 1 ml of deionized water was put back to keep the same water content. The ratio of sample to solution was 0.15 g to 100 ml. The concentration of Ca, Si, and P were also analyzed by ICP-OES.

MAS-NMR

^{29}Si magic angle spinning (MAS) NMR spectra were collected on a Varian InfinityPlus 300 MHz spectrometer operating at 59.62 MHz. A 30 s recycle delay and a 3 μs (30º tip angle) pulse were used which produced relaxed spectra. ^{29}Si spectra were referenced to tetramethylsilane (TMS) at 0 ppm.

Bioactivity

The effects of different calcium precursors and synthesis routes on the dissolution and bioactivity of glasses were investigated in a simulated body fluid (SBF) solution [33] at a pH of 7.40 at 37 °C. Aliquots of 75 mg of each powder were immersed in 50 ml of SBF and placed in an orbital shaker at 37 °C, for 2, 8, 24, 72, 168, 336 and 672 h, using an agitation rate of 120 rpm, which are the optimal conditions determined from a previous study [34]. Three samples of each glass were run per test, with the mean values reported.

Si, Ca, and P concentrations in the SBF solutions obtained after filtration (1 μm paper) were analyzed by ICP-OES. The filtered powder was rinsed with acetone to terminate any ongoing reactions, dried and then evaluated by XRD and Fourier-transform Infrared spectroscopy (FTIR) analyses for the formation of an HCA layer. XRD was carried out with a PANalytical X'Pert Pro MPD series automated diffractometer, using a step scanning method with Cu Kα radiation, at 40 kV and 40 mA, with a 0.040° 2θ step and a count rate of 50 s per step, for 2θ values of 5° to 75°. FTIR spectra were obtained with a Bruker Vector 22 thermal gravimetric-infrared spectrometer (TGA-IR). Glass samples were finely ground with potassium bromide (KBr) in a 1 to 100 weight

ratio and pressed into pellets. The sample was measured in transmission mode with a wavelength of 633 nm and in the range of 400 to 1600 cm^{-1}.

3. Results and Discussion

3.1 Composition

In pilot studies, calcium acetate was tested as a potential calcium source. Previously it was used as a post-treatment solution rather than a calcium precursor [35]. Here, the calcium acetate caused rapid gelation without the need for HF, but the calcium acetate precipitated during drying, leaving visible deposits on the samples. No further investigation of the use of calcium acetate was carried out.

The compositions, determined by the lithium metaborate fusion dissolution method, of the sol-gel glasses synthesized with the calcium nitrate, calcium chloride and CME, all stabilized at 700 °C are given in Table 2. All the compositions were within 1-2% of the nominal composition. This indicates that each of the calcium sources provided sufficient calcium, but it does not show whether the calcium was incorporated into the silica network.

Table 2. Compositional analysis of the sol-gel glass stabilised at 700 °C as determined by the lithium metaborate fusion dissolution and ICP.

Samples	**SiO_2**	**CaO**
70S30C nominal	70	30
70S30C-$Ca(NO_3)_2$	69.9	30.1

70S30C-$CaCl_2$	71.3	28.7
70S30C-CME	70.7	29.3

3.2. Surface area and pore size

Table 3 summarizes the mean specific surface area (SSA) and modal pore diameter (d_{mode}) data of the samples. The composition, final processing temperature and calcium precursor used all affected the pore size and SSA. Due to results of previous studies in the literature [13, 14], it was known that calcium is not incorporated into the silica network at when the gels are only dried at 60 °C, therefore these samples were not synthesized. The 70S30C glasses made with calcium nitrate and stabilized at 700 °C (traditional sol-gel processing) had a SSA of 158 m^2g^{-1} and a d_{mode} of 17.5 nm. The addition of HF not did affect these values. After sintering at 800 °C, the SSA and d_{mode} for the HF free samples decreased due to further cross-linking of the SiO_2 network under viscous flow of the glass during sintering. Sintering the samples made with HF did not change the pore size, although the SSA decreased from 156 m^2g^{-1} to 58 m^2g^{-1}. When calcium chloride was used instead of calcium nitrate in glasses stabilized at 700 °C, the SSA reduced to 44.8 m^2g^{-1} from 158 m^2g^{-1} but the d_{mode} was similar (17 nm). As the sintering temperature increased to 800 °C, the pore size was no longer measureable by the BJH method, due to low adsorption of N_2, i.e. there were no pores present or they were very small (< 2 nm). This was due to densification by viscous flow. When HF was used, the SSA decreased to less than 20 m^2g^{-1} for sintering temperatures above 700 °C.

An aim of using calcium chloride was that it could be used for low temperature synthesis, therefore samples with a final processing (drying) temperature of 60 °C were synthesized; which had a SSA of 13.3 m^2g^{-1} but no measurable pores. Monoliths could not be produced due to

excessive cracking, due to the low porosity making drying difficult. Adding the HF increased the pore size, increasing the SSA to 75.6 m^2g^{-1} and d_{mode} to 17.5 nm, reducing cracking. The effect of HF in the gelation process was also assessed from ^{29}Si MAS NMR spectroscopy (section 3.4.1). It therefore seems that the calcium chloride crystals fill the interstitial pores between silica nanoparticles that fuse together during silica network formation, and the calcium does not enter the silica network. XRD data (section 3.4.2) showed the crystals to be present.

Table 3. Surface area and modal pore diameter data collected from N_2 sorption of materials synthesized with different calcium precursors, with and without HF and with different final processing temperatures.

Samples	**70S30C $Ca(NO_3)_2$**		**70S30C $CaCl_2$**		**70S30C CME**	
Dried at 60°C	**no HF**	**HF**	**no HF**	**HF**	**no HF**	**HF**
Surface Area (m^2/g)	n/a	n/a	13.3	75.6	394.1	326.5
Modal Pore Diameter (nm)	n/a	n/a	-	17.5	9.5	12.4
Stabilised at 700°C	**no HF**	**HF**	**no HF**	**HF**	**no HF**	**HF**
Surface Area (m^2/g)	157.8	155.7	44.8	17.7	337.5	122.7
Modal Pore Diameter (nm)	17.5	17.4	17.6	17.2	9.6	7.8
Sintered at 800°C	**no HF**	**HF**	**no HF**	**HF**	**no HF**	**HF**
Surface Area (m^2/g)	62.0	58.0	31.1	15.3	31.8	47.5
Modal Pore Diameter (nm)	12.4	17.2	-	-	3.4	5.6

In contrast, using CME with a final drying temperature of 60 °C produced 70S30C gels with a SSA of 394 m^2g^{-1} and a d_{mode} of 9.4 nm. Adding HF caused a small increase in d_{mode} to 12.4 nm. After thermal stabilization of the glass at 700 °C, the SSA and d_{mode} changed relatively little (338

m^2g^{-1} and 9.6 nm respectively), indicating little change of structure as temperature increased and a glass more similar to the established 70S30C glasses made with calcium nitrate than to those made with calcium chloride. Nanopores form during the sol-gel process due to the disruption of the silica network, e.g. by calcium, and consequent evaporation of the liquid by-products of condensation (gelation). The presence of nanopores and the similar SSA and d_{mode} values between gels dried at 60 °C and glasses stabilized at 700 °C indicate that the calcium is integrated into the silica network at low temperature. Sintering the glasses made with CME had a dramatic effect, reducing SSA and d_{mode} to 47.5 m^2g^{-1} and 3.4 nm respectively. HF had little effect when the glasses were sintered at 800 °C.

3.3 XRD of glasses stabilized at 700°C

It is important that the new synthesis methods do not cause crystallization of the silica network as this would change the bioactivity of the materials. Previous work has shown 70S30C made with calcium nitrate to be amorphous after heating above 400 °C and below 850 °C [14]. Below 400 °C, XRD showed calcium nitrate to be present, indicating the calcium was not incorporated. Above 850 °C, the glass crystallized to wollastonite [14]. Figure 2 shows XRD patterns for glasses stabilized at 700 °C with the different calcium precursors. Figure 2 shows that using calcium chloride caused phase separation (associated with peaks which could not be identified), indicating that calcium chloride is not a suitable calcium source. However, materials synthesized with CME were amorphous.

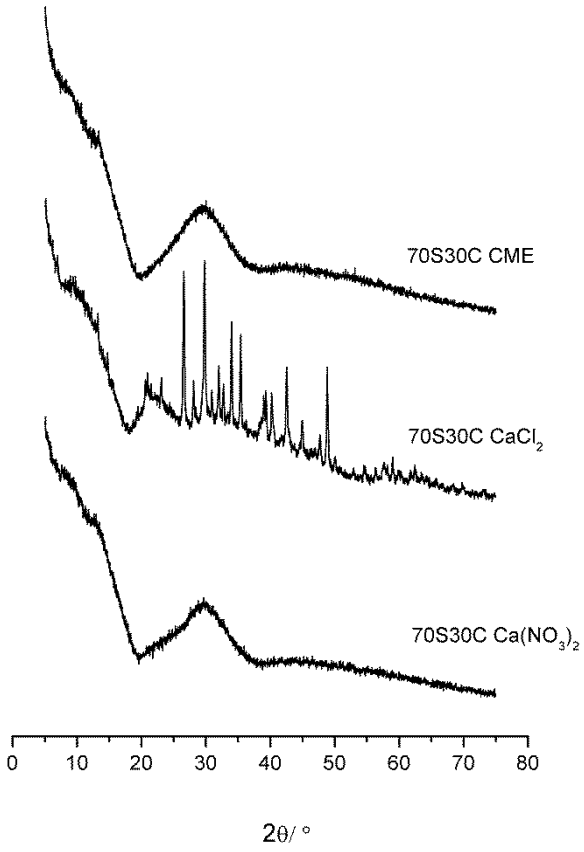

Figure 2. XRD patterns of as-synthesized bioactive glass samples after stabilization at 700 °C, made with different calcium precursors: Calcium nitrate ($CaNO_3$); calcium chloride ($CaCl_2$) and calcium methoxyethoxide (CME).

Sintering at 800 °C did not cause further structural changes in any of the samples (data not shown). It is therefore worth investigating further the temperature at which the calcium enters the silica network during the process when CME is used, and whether there is potential for its use in the low temperature synthesis regimes required for the synthesis of hybrids. It is also important to determine whether glasses and gels formed with CME can form an apatite layer in SBF.

3.4 Effect of calcium precursor on calcium incorporation

3.4.1 NMR

^{29}Si MAS NMR spectroscopy provides data on the structural changes due to calcium incorporation and heat treatment by determining the distribution of silicon Q^n species. Q^n species are silicon atoms connected to other silicon atoms by n bridging oxygens (oxygen atoms covalently bonding to two silicon atoms forming Si-O-Si bonds). Q^n corresponds to the structures of $Si(OSi)_n(OR)_{4-n}$, where OR is a non-bridging oxygen (NBO) which can either be a hydroxyl (R = H) or is a negatively charged oxygen (no R) which then correspond to Q^n(H) or Q^n(Ca) species [36-38]. In the 70S30C sol-gel derived glasses, the presence of both Q^n(H) and Q^n(Ca) made the spectra deconvolution and specific peak assignment difficult. In this paper Q^n species can have contributions from both H^+ (as an OH) and Ca^{2+} as charge-balance for NBOs.

^{29}Si MAS NMR spectra of 70S30C samples synthesized from the three precursors and thermally treated at different temperatures are shown in Figure 3. To quantify the Q^n distribution the ^{29}Si MAS NMR spectra were deconvoluted by Gaussian fitting using DMFIT software [39] and the results are shown in Table 4.

Our previous work showed that for 70S30C glasses synthesized from calcium nitrate, calcium was incorporated in the silicate network during the stabilization process (at >400 °C) [14]. Following drying at 130 °C, there was a well polymerized silica network (69 % Q^4, 27% Q^3 and 4% Q^2) [7]. Stabilizing at 600 °C caused a decrease in Q^4 to 36% [7], due to incorporation of calcium reducing the number of Si-O-Si bonds and increasing the number of non-bridging oxygen bonds. The percentage of Q^3 was similar, but calcium incorporation was reflected as the amount of Q^2

increased to 16%, with Q^1 and Q^0 species appearing (17% and 8% respectively) [14].

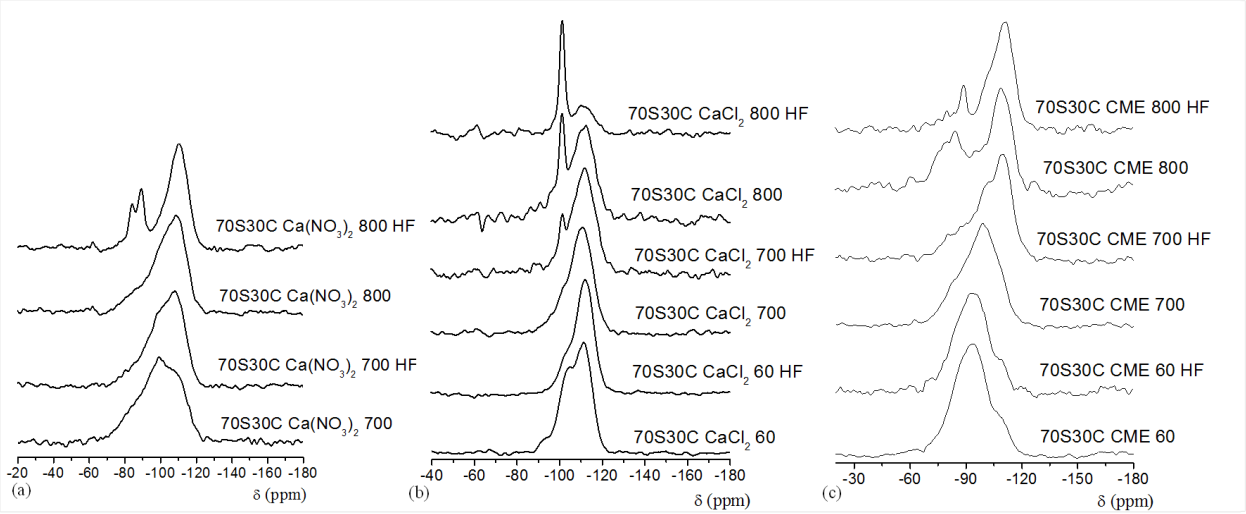

Figure 3. ^{29}Si solid state MAS-NMR spectra of 70S30C gels as a function of final processing temperature, following synthesis with (a) calcium nitrate ($CaNO_3$); (b) calcium chloride ($CaCl_2$) and (b) calcium methoxyethoxide (CME), all with and without the use of HF.

Table 4 shows that increasing the temperature to 700 °C caused a small amount of densification of the silica network with the percentage of Q^4 increasing to 40%. When the glass was sintered at 800 °C the amount of Q^4 increased to 53% and Q^2 species decreased to 14%. Q^3 species seem to remain the same as for the glass sintered at 700 ºC. This behavior can be explained by the fact that structural densification starts as the glass approaches glass transition temperature (T_g). T_g was previously measured as 717 ºC [8]. Consequently, viscous flow occurs between 700 and 800 ºC resulting in structural densification (i.e. increased connectivity) of the silicate network.

Table 4 ^{29}Si MAS NMR data, giving the spectral deconvolution into different Q^n species.

Sample	Q^0			Q^1			Q^2			Q^3			Q^4		
70S30C	δ (ppm)	FWHM (ppm)	I (%)	δ (ppm)	FWHM (ppm)	I (%)	δ (ppm)	FWHM (ppm)	I (%)	δ (ppm)	FWHM (ppm)	I (%)	δ (ppm)	FWHM (ppm)	I (%)
$Ca(NO_3)_2$ 700	-	-	-	–79.5	11.4	10	–90.0	12.4	24	–98.8	10.1	26	–109.1	13.6	40
$Ca(NO_3)_2$ 700 HF	-	-	-	–81.0	10.5	6	–90.0	10.7	12	–98.8	10.7	30	–108.9	12.1	52
$Ca(NO_3)_2$ 800	-	-	-	–81.1	11.1	7	–90.7	11.3	14	–100.1	10.2	26	–109.8	11.8	53
$Ca(NO_3)_2$ 800 HF	-	-	-	–78.9	6.8	3	–89.1[b] –84.0[a]	4.4 4.0	12 9	–100.3	13.2	17	–110.7	11.5	59
$CaCl_2$ 60	-	-	-	-	-	-	–93.2	6.4	5	–102.8	7.9	35	–111.5	9.2	60
$CaCl_2$ 60 HF							–95.0	4.9	1	–102.7	7.7	18	–112.2	9.6	81
$CaCl_2$ 700	-	-	-	-	-	-	–94.3	7.4	5	–101.1	7.3	13	–110.9	11.4	82
$CaCl_2$ 700 HF	-	-	-	-	-	-	–97.0	5.8	2	–	2.5	5	–	11.4	77

										101.2[d] – 103.1	11.5	16	112.1		
$CaCl_2$ 800	-	-	-	-	-	-	–95.1	9.3	8	– 101.4[d] – 100.7	2.6 8.2	11 15	– 112.3 – 106.1	10.2 5.5	60 6
$CaCl_2$ 800 HF	-	-	-	-	-	-	-	-	-	– 101.1 – 101.1[d]	7.2 2.6	26 34	– 111.7	9.6	40
CME 60	–76.6	11.3	10	–85.3	9.1	23	–92.4	9.1	29	–98.6	9.1	22	– 108.2	11.1	16
CME 60 HF	–73.4	11.1	7	–83.6	8.8	18	–91.8	10.1	39	–99.1	8.4	23	– 108.3	9.4	13
CME 700	–75.4	8.4	5	–82.6	7.8	12	–90.1	9.2	19	–98.9	10.7	43	– 108.0	9.9	21
CME 700 HF	–76.5	6.6	4	–83.6 –79.9[c]	5.8 2.8	6 1	–92.0 –89.8 b –87.2	8.1 2.3 3.0	10 1 2	–99.8	8.6	23	– 110.0	11.3	53

							b								
CME 800	–71.8	9.2	4	–78.8	10.6	17	–88.5 –84.2 [a]	10.2 4.4	11 5	–97.1	9.9	11	–109.5	12.3	52
CME 800 HF	–68.7	5.2	2	–79.8[c] –75.6	3.1 4.2	2 2	–92.0 –88.6 –83.8	6.1 3.8 3.8	4 3 2	–99.8	8.6	23	–111.2	10.8	61

FWHM, δ and I represent the linewidth full-width half-maximum, ^{29}Si chemical shift and relative intensity, respectively.

Errors associated with measurements are - FWHM ± 1 ppm, δ ± 2 ppm and Integral ±2%.

[a] Q^2(Ca) in three-ring silicate ions in α-$CaSiO_3$ (pseudo-wollastonite)

[b] Q^2(Ca) in chain silicate ions in β-$CaSiO_3$ (wollastonite)

[c] Q^1(Ca) in cuspidine, $Ca_4Si_2O_7F_2$

[d] unidentified crystalline phase, probably based on Q^3

For glasses sintered at 800 ºC, Figure 3 shows that the presence of fluoride ions (due to use of HF as a catalyst) leads to the formation of crystalline calcium silicate crystalline phases as is evident in the spectrum of 70S30C-Ca$(NO_3)_2$-800 HF sample (Figure 3a). This is because the Q^2(Ca) species in this sample exist in two environments. The chemical shifts at –84.0 ppm and –89.1 ppm are assigned to Q^2(Ca) environments in α-$Ca_3Si_3O_9$ ring metasilicate (pseudo-wollastonite) and β-$Ca_3Si_3O_9$ chain phases (wollastonite) which separate from the silicate network [40].

Figure 3b and Table 4 show that when $CaCl_2$ was used, calcium did not enter the silicate network at low processing temperature (60 ºC). The silica network was well polymerised as suggested from the dominance of Q^4 (60%) and Q^3 species (35%). The percentage of Q^4 species was higher than for glasses synthesized with calcium nitrate (36%), indicating that calcium was not incorporated into the silica network, even at 700 °C. When HF was used as the catalyst the concentration of Q^4 species increased (81%) and Q^3(H) decreased (18%). This is due to the HF increasing the rate of condensation, causing formation of highly branched clusters and the gelation by linking of the clusters, producing a highly cross-linked silica network. Increasing the temperature to 700 ºC in the HF-free gel lead to further condensation between silanols which strengthened the silica network with an increase of the Q^4 concentration (60% to 82%) and a correspondingly decrease (35% to 13%) of Q. Q^2 was just 5%, indicating that little calcium was incorporated into the silicate network at 700 ºC (Q^2 was 24% when calcium nitrate was used). A further increase of the temperature to 800 ºC leads to some phase separation with the peaks around –101 ppm. The peak position does not correspond to a known crystalline calcium silicates. Calcium does not seem to enter the silica network even at 800 ºC as the Q^n(Ca) species

of lower connectivity are absent and the concentration of Q^2 is low. Therefore calcium chloride is not a suitable calcium precursor for low or high temperature sol-gel synthesis.

For 70S30C samples synthesized by the alkoxide (CME and TEOS) route, the distributions of Q^n structures was very different to the gels made with calcium salts (Figure 3c and Table 4). When the gels were dried at 60 ºC they had 16% Q^4, 22% Q^3, 29% Q^2, 23% Q^1, 10% Q^0, indicating the calcium was well distributed throughout the silica network, reducing the number of bridging oxygen bonds and increasing the number of non-bridging oxygens. Condensation reactions between $(OC_2H_5)_3SiOH$ and $HOCa(OCH_2CH_2OCH_3)$ obtained from the hydrolysis of TEOS and CME, take place in the early steps of the gel formation and form $SiO^- Ca^{2+} {}^-OSi$ non-bridging oxygens (NBOs). This explains the low concentration of Q^4 species even at 60 ºC, because calcium is incorporated in the silicate matrix below this temperature. At this stage there seems to be a very small difference between samples synthesized with and without HF.

Increasing the temperature to 700 ºC, increased formation of new siloxane bridges and silanols, shown by the slight increase in Q^4 and Q^3 species. When structural densification occurred at 800 ºC, separation α-$CaSiO_3$ was observed.

When F^- ions were present and the gels were stabilized at 700 ºC, the concentration of Q^4 species increased substantially to 53% compared to 21% without HF, while the concentration of the silicate tetrahedra of lower connectivity (Q^3) decreased to 10% compared to 19% without HF. This could be due to the presence of the fluoride causing the structural densification to occur earlier with rapid formation of the silicate network. When fluoride was present, separation of

silicate phases occurred at 700 ºC, which would account for the reduction in surface area when HF was used (Table 3), whereas a temperature of 800 ºC was needed for this to occur without HF. It seems that when fluorine is involved, a chain configuration of $CaO{\cdot}SiO_2$ is preferred compared with the sample without fluorine where rings were found. The peak at –80.0 ppm can be assigned to silicon tetrahedra in the Q^1(Ca) configuration in cuspidine ($Ca_4Si_2O_7F_2$), which can be formed at this temperature due to the affinity of fluorine for calcium ions and early formation of CaF_2. This species has a reported chemical shift of –79.9 ppm [41]. As fluoride ions are at relatively low concentration the amount of this phase is small (1-2%). This phase has been also detected in the literature in the melt-quench synthesized samples containing CaF_2 [42]. When F^- ions are present in the system the structural densification seems to occur earlier. However, crystallization of calcium silicates does not take place until 800 °C, when phase separation occurs giving rise to cuspidine and wollastonite.

The NMR data suggest that CME is an ideal calcium source for low temperature sol-gel synthesis. It was then important to determine how using CME affects calcium ion release in solution and whether glasses made with CME were bioactive in SBF.

3.4.2 XRD as a function of calcium source and temperature

Figure 4 shows the X-ray diffraction data for samples with different Ca precursors as a function of final thermal processing temperature, and dissolution data in deionised water for samples with specially chosen stabilization temperatures. The aim was to investigate how the final processing temperature affected calcium incorporation and consequently calcium release. Water was chosen because SBF contains calcium.

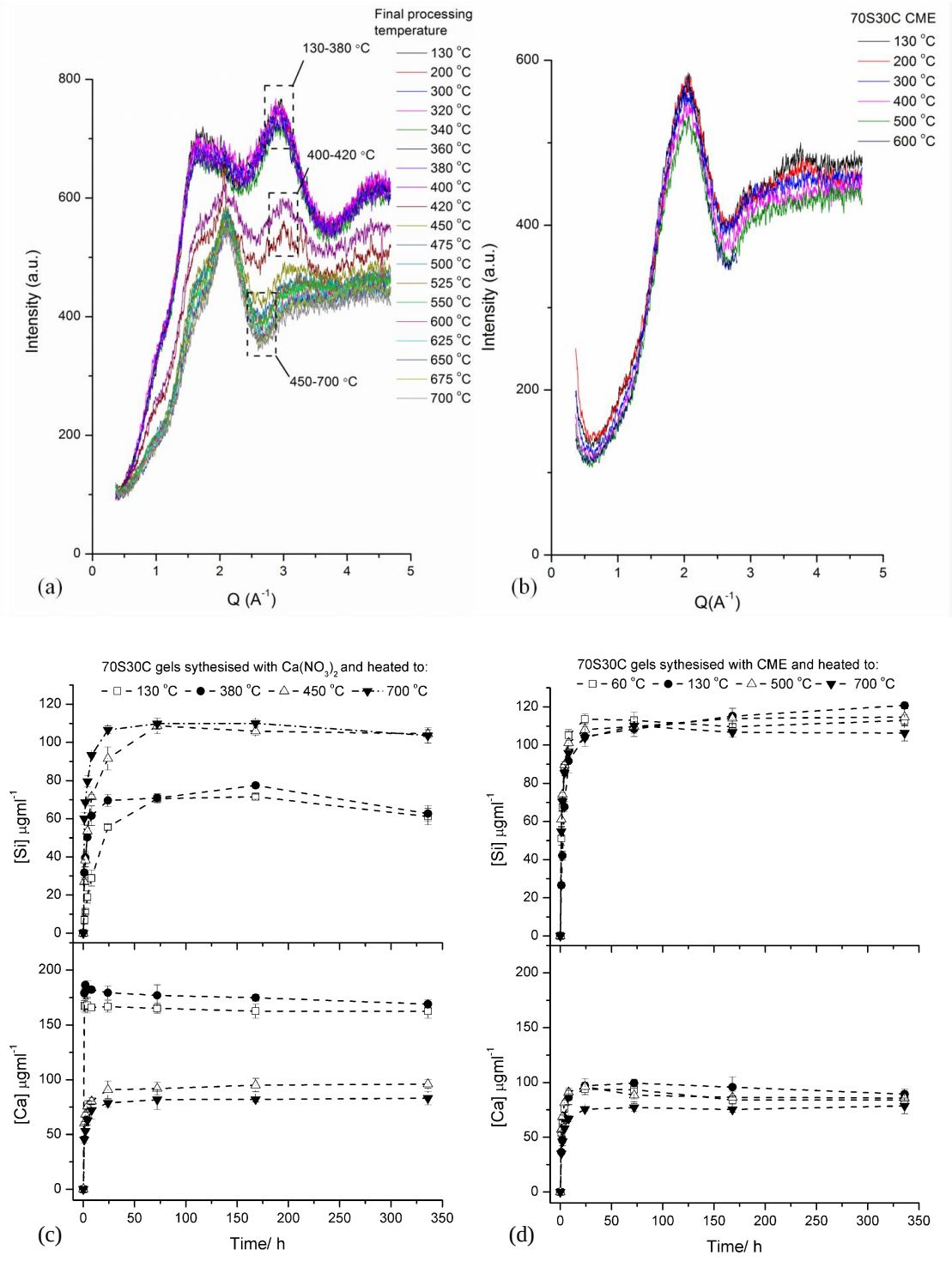

Figure 4. (a,b) X-ray diffraction patterns of 70S30C gels as a function of final processing temperatures using (a) calcium nitrate ($CaNO_3$); (b) calcium methoxyethoxide (CME); (c, d) dissolution profiles of 70S30C gels following different final processing temperatures.

Figure 4a shows the diffraction patterns for the 70S30C sample prepared using the $Ca(NO_3)_2 \cdot 4H_2O$ precursor. The patterns can be divided into three categories as follows. The first subset, which show two clear principal peaks, correspond to the as-prepared 70S30C prior to heat treating through to samples heat treated up to 380 °C. The second subset corresponds to samples heat treated to 400 °C and 420 °C and reveals a transitional profile between the first and third subsets. The third subset, which has a single principal peak at Q = 2.1 $Å^{-1}$, corresponds to samples heat treated above 450 °C and up to 700 °C, which is below T_g and the onset of crystallization. The diffraction pattern for this third subset is consistent with previously published diffraction data [13, 14], attributed to the nitrate decomposing and calcium entering the glass network. The patterns suggest that the calcium begins to enter and disrupt the silica network at 400 °C and is fully incorporated at 450 ˚C. The temperatures selected for dissolution tests were therefore: 130 °C (usual drying temperature of gels prior to thermal stabilization), 380 °C (immediately before calcium incorporation), 450 °C (immediately after calcium incorporation) and 700 °C (stabilization temperature below T_g). Figure 4c and 4d show the corresponding dissolution profiles in deionized water. Samples heated to 380 °C or less released calcium very rapidly (179 $\mu g ml^{-1}$ within 2 h). In contrast, samples heated above 450 °C only released 83 $\mu g ml^{-1}$ (after heating to 450 °C) of calcium ions and 96 $\mu g ml^{-1}$ (after heating to 700 °C) after 2 weeks immersion. These results show that, as anticipated, calcium did not incorporate into the network until > 380 °C. The silica release data supports this as samples heated to ≤ 380 °C released less silica than those that incorporated the calcium in the network because without the calcium incorporated, the silica network has a higher connectivity which is more resistant to corrosion. The ^{29}Si MAS NMR data support this hypothesis (Figure 3 and Table 4).

XRD (Figure 2) and ^{29}Si NMR data for glasses synthesized with $CaCl_2$ indicated that the calcium was never incorporated into the silica network (Figure 3 and Table 4) and the dissolution rate of calcium in the distilled water was approximately 200 $\mu g ml^{-1}$ after 2 h immersion for samples dried at 130 °C and stabilized at 500 °C (data not shown).

Figure 4b shows the diffraction patterns for the 70S30C sample prepared using the CME precursor. There was no change in the diffraction pattern following heat treatment with increasing temperatures. A single principal peak occurs at Q = 2.1 $Å^{-1}$ showing that calcium has already entered the glassy network at 130 °C [13]. Dissolution tests were run at 60 °C (drying temperature of hybrids) and 130 °C (drying temperature prior to stabilization of glasses), 500 and 700 °C (the thermal stabilization temperature for glasses below T_g). Figure 4d shows the dissolution profiles, which indicate that all the samples have very similar release rates of soluble silica and calcium, independent of the final processing temperature. Comparison with Figure 4c shows that the release rate of calcium was similar to that from the glass sample synthesized with calcium nitrate and heated to 700 °C. This supports the hypothesis that calcium entered the silica network below 60 °C. It is important to determine whether gels and glasses made with CME have the potential to be bioactive.

3.5 Bioactivity testing

Using CME allowed incorporation of calcium at low temperature. It was therefore important to determine whether the gel and glass made with CME can be considered bioactive. Figure 5 shows the XRD patterns of materials synthesized with CME as a function of drying or stabilization temperature and of each material following 4 weeks immersion in SBF. The patterns

from samples synthesized without HF were amorphous at all final processing temperatures, even though the NMR data suggested some crystallization occurred after sintering at 800 °C. Gels synthesized with HF and dried at 60 °C contained small Bragg peaks representing CaF_2 (28°, 47°, 56°, and 69°). This was attributed to the HF reacting with Ca from CME to form CaF_2. This is not of significant concern as the amount of fluoride used in the process is low; indeed, fluoride-releasing bioactive glasses are themselves of interest in both orthopedic and dental applications as they can form fluorapatite [42, 43]. When the gels were heated to 700 °C, the CaF_2 formed cuspidine ($Ca_4Si_2O_7F_2$). Samples not synthesized with HF remained XRD amorphous at all temperatures. All spectra that were collected from samples after 4 weeks immersion in SBF had peaks corresponding to HCA, indicating potential for bioactivity; however, the relative intensity of the HCA peaks decreased as the sintering temperature was increased from 700 to 800 °C. This is likely to be due to densification of the silica network and the driving off of -OH groups (Table 4) which act as network modifiers to the silica network and nucleation sites for HCA. For potential hybrid synthesis, it is encouraging to see amorphous spectra after drying at 60 °C and even more encouraging to see HCA formation after immersion in SBF.

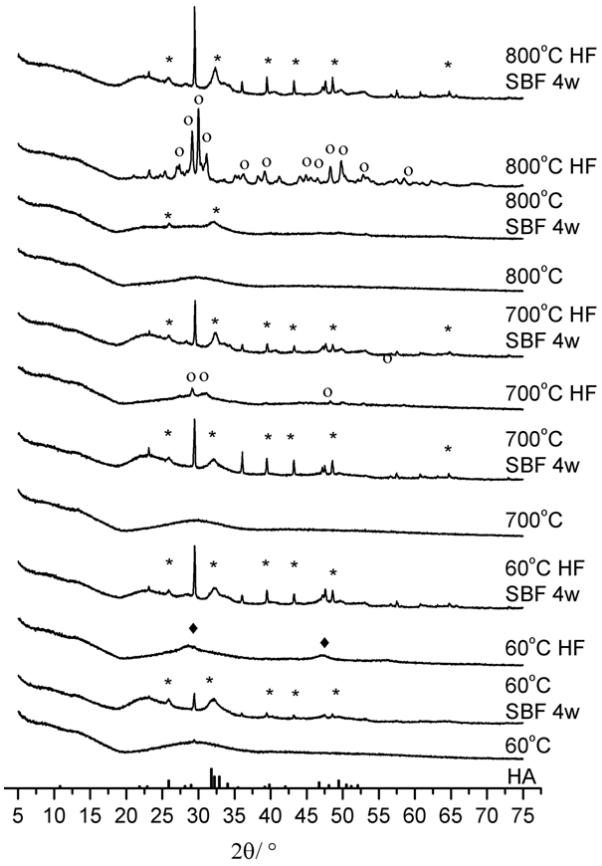

Figure 5. XRD patterns of 70S30C synthesized using calcium methoxyethoxide (CME) with different final processing temperatures and after reaction in SBF for 4 weeks, (*) signifies the crystals of hydroxyapatite, (°) signifies the crystals of cuspidine, and (♦) signifies crystals of calcium fluoride. The XRD pattern of hydroxyapatite powder is also included for reference.

HCA formation after 4 weeks in SBF is not enough to suggest bioactivity. If CME is to be used in bioactive hybrid synthesis, it is important that the gels made with CME and dried at 60 °C form an HCA layer in SBF in less than 1 week. Figure 6 shows FTIR spectra and XRD patterns of 70S30C gels synthesized with CME and dried at 60 °C (without HF) after different immersion times in SBF. The FTIR spectrum of the unreacted gel (Figure 6a), before immersion, contains vibration bands (875 and 1400 cm^{-1} which are C-O stretching and bending modes

respectively) corresponding to the formation of surface carbonates. The splitting of ~100 cm^{-1} of ν_3 vibration indicates the formation of monodentate carbonates. Figure 6a shows that within 2 h of immersion, a broad absorbance band (550-600 cm^{-1}) often attributed to amorphous phosphate species was present [44]. After immersion for 24 h the P-O bending bands that are associated with orthophosphate (571 and 602 cm^{-1}) evolved. The vibration corresponding to $\delta_{Si\text{-}O\text{-}Si}$ at 800 cm^{-1} increased in intensity after the sample was immersed in SBF, suggesting the formation of silica-rich layer. After 24 and 72 h of immersion, the reappearance of vibration bands at 1410 cm^{-1} and 870 cm^{-1} indicate a B type carbonate substitution in HA, while the vibration at 1460 cm^{-1} is for an A substitution. Therefore an AB carbonate substituted apatite is formed, indicative of HCA. XRD patterns (Figure 6b) show crystalline peaks that can be assigned to HCA (2θ value of approximately 31°) are present after 24 h immersion. A small peak was present at 8 h. These results indicate that CME can produce bioactive gels. Calcite was also detected in the XRD patterns after 24 h immersion.

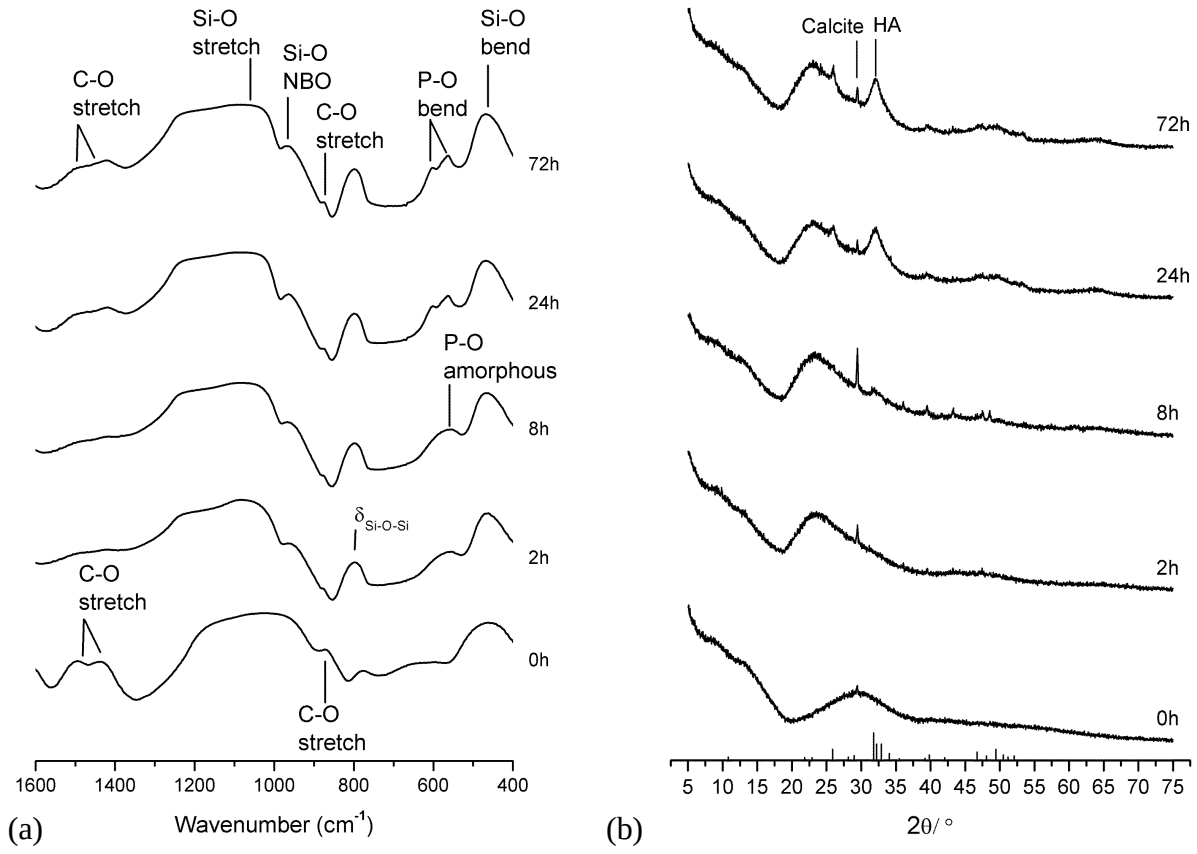

Figure 6. 70S30C gel synthesized with CME and dried at 60 °C after immersion in simulated body fluid as a function of time: (a) FTIR (b) XRD, including the XRD pattern of HA.

Figure 7a shows the release profiles in SBF of soluble silicon, calcium and phosphorus species from gels made with CME and $CaCl_2$ precursors and dried at 60˚C. Over the first week of immersion in SBF, the calcium content of the SBF was approximately 50 μgml^{-1} higher (257.3 μgml^{-1}) for samples synthesized with CME compared to those synthesized with $CaCl_2$ (206.8 μgml^{-1}). This is either due to the samples made with CME releasing more calcium ions, or due to the gels made with $CaCl_2$ nucleating more calcium species, e.g. HA. The phosphorus content of the SBF decreased rapidly after the gels were immersed, from 33 μgml^{-1} to around 10 μgml^{-1}, and all the phosphorus was removed from the SBF by 72 h, indicating possible calcium

phosphate nucleation, which is in line with the XRD and FTIR data (Figure 6). Dissolution profiles of samples gelled with HF were very similar (data not shown).

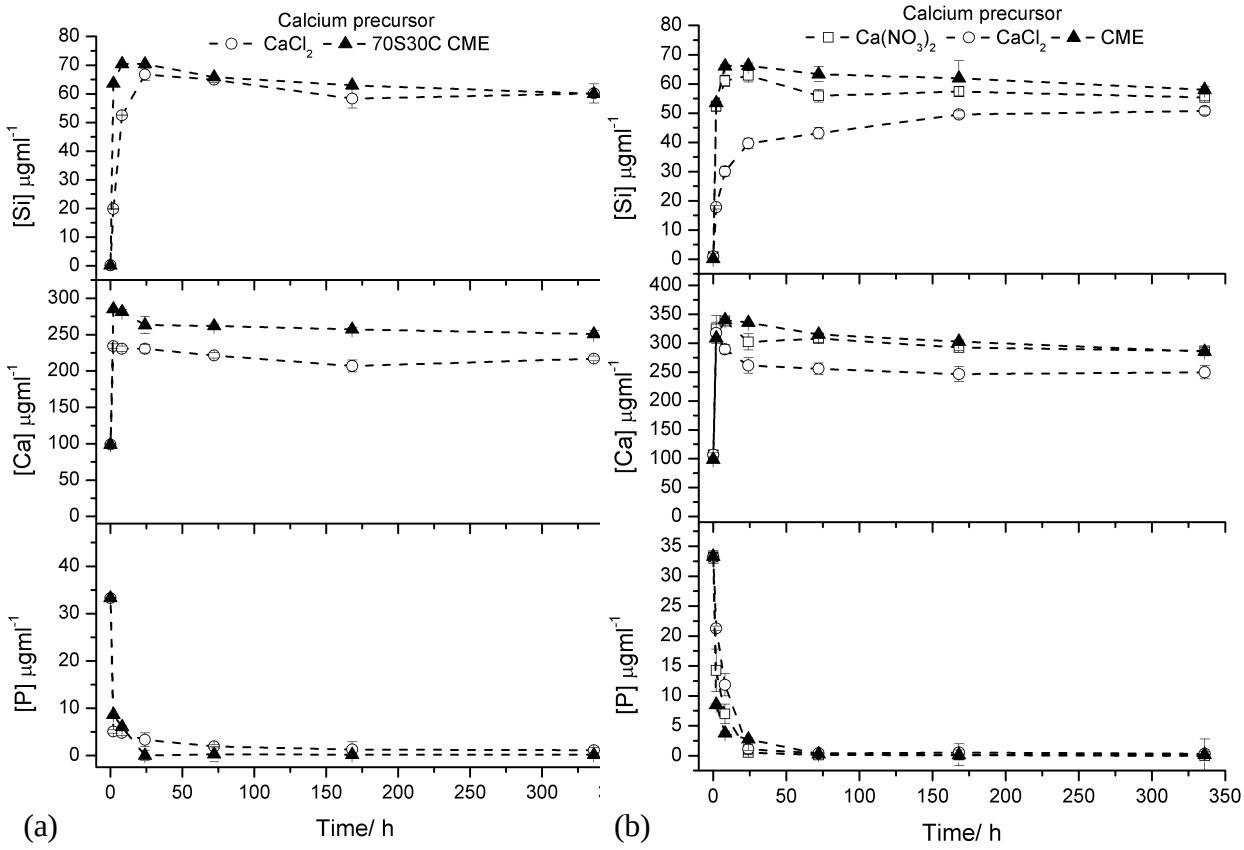

Figure 7. ICP data of simulated body fluid after immersion of 70S30C gels synthesized with different calcium precursors and using different final processing temperatures of (a) 60 °C and (b) 700 °C.

Figure 7b shows the dissolution profiles in SBF following immersion of the glasses stabilized at 700 °C. The silica release rate was slightly lower than for the gels. The glasses synthesized with calcium chloride had the lowest release rate of soluble silica (around 30 μgml^{-1} after 8 h). The reason for this is that the glasses synthesized with calcium chloride had SSA values up to an

order of magnitude smaller than those made with calcium nitrate or CME and due to the higher percentage of Q^4 units (approximately double that of the other glasses). Glasses made with either calcium nitrate or CME had similar dissolution rates, with CME glasses slightly higher at approximately 70 μgml^{-1} after 8 h. The reason for the higher dissolution of CME glasses is attributed to their higher SSA (Table 3). The phosphorus concentration in the SBF decreased rapidly immediately after immersion for all samples, reaching zero by 24 h, indicating possible HCA formation. For the glasses that were gelled with HF, the release profiles showed similar trends (data not shown) except that the silica and calcium ion release rates were slightly lower, e.g. 70S30C synthesized with CME, silica release was 52.1 μgml^{-1} after 8 h for glasses gelled with HF compared to 66.1 μgml^{-1} for glasses gelled without HF. This is due to the significant decrease of surface area from ~340 m^2g^{-1} (without HF) to 120 m^2g^{-1} (with HF). When the glasses were sintered to 800 °C, the dissolution of the glasses decreased, e.g. 70S30C synthesized with CME released 31.5 μgml^{-1} of soluble silica after 8 h immersion when sintered at 800 °C compared to 66.1 μgml^{-1} when stabilized at 700˚C. This is again likely to be due to densification of the silica network (Table 4) and associated SSA decrease from 340 m^2g^{-1} to 32 m^2g^{-1} during sintering at 800 °C. As a result of this, the phosphate precipitation within the SBF was slower, indicating slower HCA formation (which seems to form at around 3 days of immersion).

4. Summary

CME seems to be an excellent alternative to calcium salts for incorporation of calcium into the silica network at processing temperatures below 60 °C. The hypothesis for the mechanism of incorporation of the calcium is that the CME hydrolyses when it is added to the hydrolyzed TEOS sol and incorporates calcium into the wet gel. As gelation and drying proceed, the silica

network continues to cross-link but maintains the calcium in the network. In contrast, when calcium salts are used they remain in solution until drying, only being incorporated when they are broken down thermally at high temperature, or in the case of calcium chloride, not at all. The use of calcium nitrate in the sol-gel process has recently been shown to cause inhomogeneity in the calcium distribution [12, 15]; CME is therefore a promising alternative for the production of more homogeneous glasses and in the synthesis of sol-gel hybrid materials containing organic polymers.

5. Conclusions

The results confirm the earlier observation that when sol-gel glasses are synthesized with calcium nitrate, the calcium only enters the network above ~400 ˚C. When calcium chloride is used as an alternative, calcium is not incorporated at any temperature. Calcium salts are therefore not useful calcium sources for the low temperature (~60 ˚C) synthesis regimes required for glass-polymer hybrids. Calcium was found to enter the glassy network during the drying process for 70S30C prepared using CME. The use of HF as a gelation catalyst did not affect calcium incorporation, although some calcium fluoride was formed. Heating the dried gels synthesized with CME to the temperatures used for stabilizing sol-gel glasses did not change the calcium dissolution or structure of the silica network. CME is therefore a suitable calcium precursor for synthesizing bioactive sol-gel glasses, low temperature gels and potentially hybrids.

Acknowledgements

JRJ acknowledges the EPSRC Challenging Engineering Scheme (EP/I02086). He was a Royal Academy of Engineering/EPSRC Research Fellow and also acknowledges support from the

Royal Society and the Philip Leverhulme Prize. The authors also acknowledge support from the EPSRC (EP/E057098/1 and EP/E050611/1). The NMR equipment used in this research received funding from EPSRC, BBSRC, the University of Warwick and Birmingham Science City Projects supported by Advantage West Midlands and the European Regional Development Fund.

References

(1) Hench, L. L.; Polak, J. M., Third-generation biomedical materials. *Science* **2002,** *295* (5557), 1014-1017.

(2) Valliant, E. M.; Jones, J. R., Softening bioactive glass for bone regeneration: sol-gel hybrid materials. *Soft Matter* **2011,** *7* (11), 5083-5095.

(3) Jones, J. R., Review of bioactive glass: From Hench to hybrids. *Acta Biomater* **2012,** *http://dx.doi.org/10.1016/j.actbio.2012.08.023*.

(4) Hench, L. L.; Splinter, R. J.; Allen, W. C.; Greenlee, T. K., Bonding mechanisms at the interface of ceramic prosthetic materials. *J. Biomed. Mater. Res. Symp.* **1971,** *5* (6), 117-141.

(5) Li, R.; Clark, A. E.; Hench, L. L., An investigation of bioactive glass powders by sol-gel processing. *J. Appl. Biomater.* **1991,** *2* (4), 231-239.

(6) Sepulveda, P.; Jones, J. R.; Hench, L. L., Characterization of melt-derived 45S5 and sol-gel-derived 58S bioactive glasses. *J. Biomed. Mater. Res.* **2001,** *58* (6), 734-740.

(7) Sepulveda, P.; Jones, J. R.; Hench, L. L., Bioactive sol-gel foams for tissue repair. *J. Biomed. Mater. Res.* **2002,** *59* (2), 340-348.

(8) Jones, J. R.; Ehrenfried, L. M.; Hench, L. L., Optimising bioactive glass scaffolds for bone tissue engineering. *Biomaterials* **2006,** *27*, 964-973.

(8) Lin, S.; Ionescu, C.; Baker, S.; Smith, M. E.; Jones, J. R., Characterisation of the inhomogeneity of sol–gel-derived SiO_2–CaO bioactive glass and a strategy for its improvement. *J. Sol-Gel Sci. Technol.* **2010,** *53*, 255-262.

(9) Hench, L. L.; Vasconcelos, W., Gel-silica science. *Ann. Rev. Mater. Sci.* **1990,** *20*, 269-298.

(10) Hench, L. L.; West, J. K., The sol-gel process. *Chem. Rev.* **1990,** *90* (1), 33-72.

(11) Brinker, J.; Scherer, G. W., *Sol-gel science : the physics and chemistry of sol-gel processing*. Academic Press: Boston, 1990.

(12) Seebach, C.; Schultheiss, J.; Wilhelm, K.; Frank, J.; Henrich, D., Comparison of six bone-graft substitutes regarding to cell seeding efficiency, metabolism and growth behaviour of human mesenchymal stem cells (MSC) in vitro. *Injury* **2010,** *41* (7), 731-738.

(13) Skipper, L. J.; Sowrey, F. E.; Pickup, D. M.; Drake, K. O.; Smith, M. E.; Saravanapavan, P.; Hench, L. L.; Newport, R. J., The structure of a bioactive calcia-silica sol-gel glass. *J. Mater. Chem.* **2005,** *15* (24), 2369-2374.

(14) Lin, S.; Ionescu, C.; Pike, K. J.; Smith, M. E.; Jones, J. R., Nanostructure evolution and calcium distribution in sol-gel derived bioactive glass. *J. Mater. Chem.* **2009,** *19* (9), 1276-1282.

(15) Yue, S.; Lee, P. D.; Poologasundarampillai, G.; Yao, Z.; Rockett, P.; Devlin, A. H.; Mitchell, C. A.; Konerding, M. A.; Jones, J. R., Synchrotron X-ray microtomography for assessment of bone tissue scaffolds. *J Mater. Sci. Mater. Med.* **2010,** *21* (3), 847-53.

(16) Bonhomme, C.; Gervais, C.; Folliet, N.; Pourpoint, F.; Diogo, C. C.; Lao, J.; Jallot, E.; Lacroix, J.; Nedelec, J. M.; Iuga, D.; Hanna, J. V.; Smith, M. E.; Xiang, Y.; Du, J. C.; Laurencin, D., Sr-87 solid-state NMR as a structurally sensitive tool for the investigation of materials: Antiosteoporotic pharmaceuticals and bioactive glasses. *J. Am. Chem. Soc.* **2012**, 134 (30), 12611-12628.

(17) Novak, B. M., Hybrid nanocomposite materials - between inorganic glasses and organic polymers. *Adv. Mater.* **1993,** *5* (6), 422-433.

(18) Mahony, O.; Tsigkou, O.; Ionescu, C.; Minelli, C.; Ling, L.; Hanly, R.; Smith, M. E.; Stevens, M. M.; Jones, J. R., Silica-Gelatin Hybrids with Tailorable Degradation and Mechanical Properties for Tissue Regeneration. *Adv. Funct. Mater.* **2010,** *20* (22), 3835-3845.

(13) Poologasundarampillai, G.; Ionescu, C.; Tsigkou, O.; Murugesan, M.; Hill, R. G.; Stevens, M. M.; Hanna, J. V.; Smith, M. E.; Jones, J. R., Synthesis of bioactive class II poly(g-glutamic acid)/silica hybrids for bone regeneration. *J. Mater. Chem.* **2010**. *20* (40), 8952-8961.

(14) Pereira, M. M.; Clark, A. E.; Hench, L. L., Calcium-Phosphate Formation on Sol-Gel-Derived Bioactive Glasses in-Vitro. *J. Biomed. Mater. Res.* **1994,** *28* (6), 693-698.

(15) Ramila, A.; Balas, F.; Vallet-Regi, M., Synthesis routes for bioactive sol-gel glasses: Alkoxides versus nitrates. *Chem. Mater.* **2002,** *14* (2), 542-548.

(16) Manzano, M.; Arcos, D.; Delgado, M. R.; Ruiz, E.; Gil, F. J.; Vallet-Regi, M., Bioactive star gels. *Chem. Mater.* **2006,** *18* (24), 5696-5703.

(17) Poologasundarampillai, G.; Yu, B. B.; Jones, J. R.; Kasuga, T., Electrospun silica/PLLA hybrid materials for skeletal regeneration. *Soft Matter* **2011,** *7* (21), 10241-10251.

(18) Pickup, D. M.; Valappil, S. P.; Moss, R. M.; Twyman, H. L.; Guerry, P.; Smith, M. E.; Wilson, M.; Knowles, J. C.; Newport, R. J., Preparation, structural characterisation and antibacterial properties of Ga-doped sol-gel phosphate-based glass. *J. Mater. Sci.* **2009,** *44* (7), 1858-1867.

(19) Mahony, O.; Tsigkou, O.; Ionescu, C.; Minelli, C.; Hanly, R.; Ling, L.; Smith, M. E.; Stevens, M. M.; Jones, J. R., Silica-gelatin hybrids with tailorable degradation and mechanical properties for tissue regeneration. *Adv. Funct. Mater.* **2010,** *20*, 3835-3845.

(20) Rhee, S. H.; Lee, Y. K.; Lim, B. S., Evaluation of a novel poly(epsilon-caprolactone)-organosiloxane hybrid material for the potential application as a bioactive and degradable bone substitute. *Biomacromolecules* **2004,** *5* (4), 1575-1579.

(21) Miyazaki, T.; Ohtsuki, C.; Tanihara, M., Synthesis of bioactive organic-inorganic nanohybrid for bone repair through sol-gel processing. *J. Nanosci. Nanotechnol.* **2003,** *3* (6), 511-515.

(22) Pereira, M. M.; Clark, A. E.; Hench, L. L., Calcium-phosphate formation on sol-gel-derived bioactive blasses in vitro. *J. Biomed. Mater. Res.* **1994,** *28* (6), 693-698.

(23) Ramila, A.; Balas, F.; Vallet-Regi, M., Synthesis routes for bioactive sol-gel glasses: Alkoxides versus nitrates. *Chem. Mater.* **2002,** *14* (2), 542-548.

(24) Manzano, M.; Arcos, D.; Delgado, M. R.; Ruiz, E.; Gil, F. J.; Vallet-Regi, M., Bioactive star gels. *Chem. Mater.* **2006,** *18* (24), 5696-5703.

(25) Poologasundarampillai, G.; Yu, B. B.; Jones, J. R.; Kasuga, T., Electrospun silica/PLLA hybrid materials for skeletal regeneration. *Soft Matter* **2011,** *7* (21), 10241-10251.

(26) Powers, K. W.; Hench, L. L., The pentacoordinate species in fluoride catalysis of silica gels. In *Sol-Gel Synthesis and Processing*, Komarneni, S.; Sakka, S.; Phule, P. P.; Laine, R. M., Eds. Amer Ceramic Soc: Westerville, 1998; Vol. 95, pp 197-206.

(27) Pickup, D. M.; Valappil, S. P.; Moss, R. M.; Twyman, H. L.; Guerry, P.; Smith, M. E.; Wilson, M.; Knowles, J. C.; Newport, R. J., Preparation, structural characterisation and antibacterial properties of Ga-doped sol-gel phosphate-based glass. *J. Mater. Sci.* **2009,** *44* (7), 1858-1867.

(28) Saravanapavan, P.; Hench, L. L., Mesoporous calcium silicate glasses. I. Synthesis. *J. Non-Cryst. Solids* **2003,** *318* (1-2), 1-13.

(29) Casoli, A.; Mirti, P., The analysis of archaeological glass by inductively coupled plasma optical-emission spectroscopy. *Fresenius J. Anal. Chem.* **1992,** *344* (3), 104-108.

(30) Brunaur, S.; Deming, L. S.; Deming, W. S.; Teller, E., On a theory of the vander waals adsorption of gases. *J. Am. Chem. Soc.* **1940,** *62*, 1723-1732.

(31) Barrett, E. P.; Joyner, L. G.; Halenda, P. P., The determination of pore volume and area distributions in porous substances. I. computations from nitrogen isotherms. *J. Am. Chem. Soc.* **1951,** *73* (1), 373-380.

(32) Sing, K. S. W.; Everett, D. H.; Haul, R. A. W.; Moscou, L.; Pierotti, R. A.; Rouquerol, J.; Siemieniewska, T., Reporting Physisorption Data for Gas Solid Systems with Special Reference to the Determination of Surface-Area and Porosity (Recommendations 1984). *Pure Applied Chem.* **1985,** *57* (4), 603-619.

(33) Kokubo, T.; Takadama, H., How useful is SBF in predicting in vivo bone bioactivity? *Biomaterials* **2006,** *27* (15), 2907-2915.

(34) Jones, J. R.; Sepulveda, P.; Hench, L. L., Dose-dependent behavior of bioactive glass dissolution. *J. Biomed. Mater. Res.* **2001,** *58* (6), 720-726.

(35) de Oliveira, A. A. R.; Ciminelli, V.; Dantas, M. S. S.; Mansur, H. S.; Pereira, M. M., Acid character control of bioactive glass/polyvinyl alcohol hybrid foams produced by sol-gel. *J. Sol-Gel Sci. Technol.* **2008,** *47* (3), 335-346.

(36) MacKenzie, K. J. D.; Smith, M. E., *Multinuclear solid state NMR of inorganic materials*. Pergamon Press: Oxford, 2002.

(37) Chuang, I. S.; Kinney, D. R.; Maciel, G. E., Interior hydroxyls of the silica-gel system as studied by Si-29 CP-MAS NMR spectroscopy. *J. Am. Chem. Soc.* **1993,** *115* (19), 8695-8705.

(38) Liu, C. H. C.; Maciel, G. E., The fumed silica surface: A study by NMR. *J. Am. Chem. Soc.* **1996,** *118* (21), 5103-5119.

(39) Massiot, D.; Fayon, F.; Capron, M.; King, I.; Le Calve, S.; Alonso, B.; Durand, J. O.; Bujoli, B.; Gan, Z. H.; Hoatson, G., Modelling one- and two-dimensional solid-state NMR spectra. *Magn. Reson. Chem.* **2002,** *40* (1), 70-76.

(40) Engelhardt, G.; Nofz, M.; Forkel, K.; Wihsmann, F. G.; Magi, M.; Samoson, A.; Lippmaa, E., Structural studies of calcium aluminosilicate glasses by high-resolution solid-state Si-29 and Al-27 magic angle spinning nuclear magnetic-resonance. *Phys. Chem. Glasses* **1985,** *26* (5), 157-165.

(41) Engelhardt, G.; Michel, D., *High-resolution solid-state NMR of silicates and zeolites*. Wiley: Chichester, 1987.

(42) Brauer, D. S.; Karpukhina, N.; Law, R. V.; Hill, R. G., Structure of fluoride-containing bioactive glasses. *J. Mater. Chem.* **2009,** *19* (31), 5629-5636.

(43) Fuji, E.; Kawabata, K.; Yoshimatsu, H.; Hayakawa, S.; Tsuru, K.; Osaka, A., Structure and biomineralization of calcium silicate glasses containing fluoride ions. *J. Ceram. Soc. Japan* **2003,** *111* (10), 762-766.

(44) Huang, S.; Ingber, D. E., The structural and mechanical complexity of cell-growth control. *Nat. Cell Biol.* **1999,** *1* (5), E131-138.

Graphical Abstract

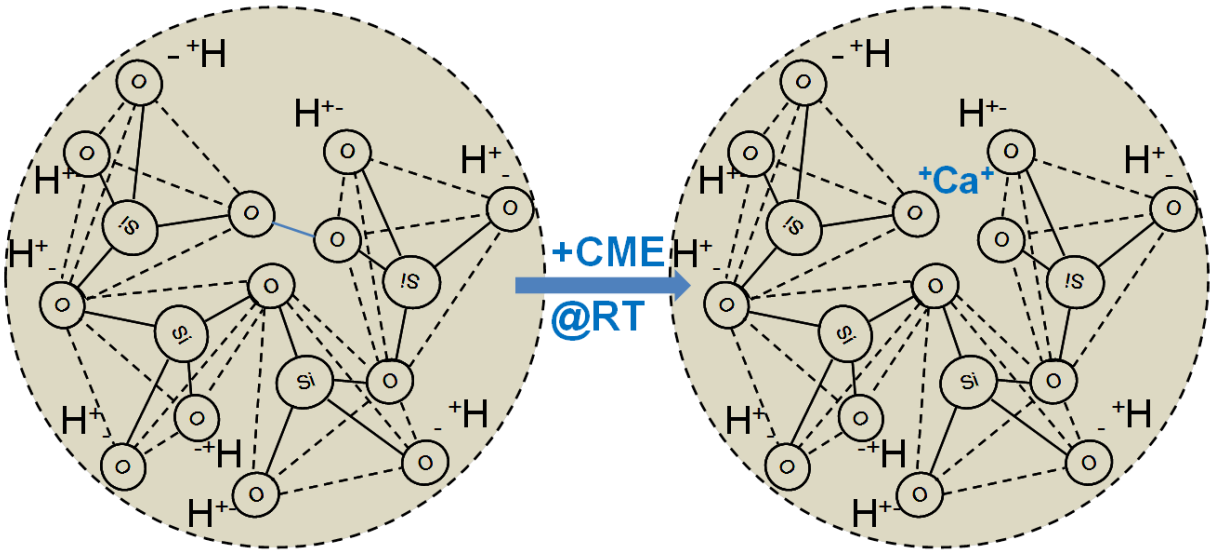

Schematic illustrating that calcium can be incorporated into the sol-gel silica network at room temperature if calcium methoxyethoxide (CME) is used as the calcium precursor. Bridging silicon-oxygen bonds are broken to incorporate the calcium. When calcium salts are used, the temperature must be raised to >400 °C for calcium incorporation to occur. The results are very important for sol-gel hybrid synthesis and for improvement of homogeneity in sol-gel glasses.